ELSEVIER

Thin Solid Films 367 (2000) 40–47

thin solid films

www.elsevier.com/locate/tsf

# Quantum dots formed by ultrathin insertions in wide-gap matrices

N.N. Ledentsov[a,1,*], I.L. Krestnikov[1a], M. Straßburg[a], R. Engelhardt[a], S. Rodt[a], R. Heitz[a], U.W. Pohl[a], A. Hoffmann[a], D. Bimberg[a], A.V. Sakharov[b], W.V. Lundin[b], A.S. Usikov[b], Zh.I. Alferov[b], D. Litvinov[c], A. Rosenauer[c], D. Gerthsen[c]

[a]*Institut für Festkörperphysik, Technische Universität Berlin, Hardenbergstrasse 36, Postfach 6980, D-10623 Berlin, Germany*
[b]*A.F. Ioffe Physico-Technical Institute, St. Petersburg, Russia*
[c]*Laboratorium für Elektronenmikroskopie der Universität Karlsruhe, Karlsruhe, Germany*

**Abstract**

We report on experimental and theoretical studies on a new type of quantum-dot (QD) structures obtained using ultrathin, i.e. below the critical thickness for 2D–3D transition, strained narrow gap insertions in wide bandgap matrices. We concentrate on submonolayer (SML) or slightly above 1 ML CdSe insertions in a wide-gap II–VI matrices and give the first results on ultrathin InGaN insertions in a GaN matrix. A discussion on detailed comparison of our original results with the results of other authors is presented. The formation of dense arrays (up to $10^{12}$ cm$^{-2}$) of nanoscale two-dimensional (2D) islands is revealed in processed high-resolution transmission electron microscopy images. In the case of stacked sheets of SML insertions, the islands in the neighboring sheets are formed predominantly in correlated or anticorrelated way for thinner and thicker spacer layers, respectively. Different polarization of photoluminescence (PL) emission recorded in edge geometry for vertically-uncoupled and coupled QDs confirms the QD nature of excitons. By monitoring of sharp lines due to single QDs using cathodoluminescence the 3D confinement is manifested. We demonstrate significant squeezing of the QD exciton wavefunction in the lateral direction using magneto-optical experiments. We point to complete suppression of lateral motion of excitons bound to islands in case of wide-gap (ZnMgSSe) matrices, as follows from PL excitation studies. A resonant (0-phonon) lasing is observed in ultrathin CdSe insertions and proves the lifting of the *k*-selection rule for QD excitons. We show that lack of exciton screening in QDs up to high excitation densities enables strong resonant modulation of the refractive index in stacked ultrathin insertions and allows realization of resonant (excitonic) waveguiding and lasing. This enables the realization of a new type of heterostructure laser operating without external optical confinement by layers having lower average refractive indices. Ultrahigh QD excitonic gain in dense arrays of stacked QDs allows a new type of surface-emitting laser. 

*Keywords:* Semiconductor low-dimensional structures; Quantum dots; Ultrathin-layer insertions in wide-gap semiconductors

## 1. Introduction

Quantum dot (QD) heterostructures [1,2], i.e. semiconductor structures providing confinement in all three dimensions, present an ultimate limit of size quantization in solids and result in the strongest possible modification of electronic properties as compared to quantum wells and wires. For laser applications, the δ-function-like density of states and the enhanced overlap of electron and hole wavefunctions in a QD result in decreased threshold current densities, higher temperature stability of the threshold current, as well as higher material and differential gain. Enhanced nonlinear effects are observed from optical properties. The recent breakthrough in device application of QDs [1] is mostly related to Stranski–Krastanow growth, resulting in the formation of three-dimensional (3D) islands on top of a wetting layer. 1.3 μm-Emitting GaAs-based lasers with parameters, superior to those in InP-based quantum well (QW) lasers are recently created [3]. With regard to this progress, there are many attempts to apply similar concept to wide-gap lasers based on II–VI material systems and group-III nitrides [4,5]. The CdSe/ZnMgSSe system represents the best choice to study physical mechanisms of lasing in wide-gap compounds and, with regard to the extended history of investigations (for a review see e.g. Ref. [6]), can be considered as a model system. For fabrication of CdSe/ZnSe QDs two principally different growth modes have been introduced. The Stranski–Krastanow mode results for the CdSe/ZnSe system in the formation of islands with a diameter being typically larger than 30 nm (e.g. Ref. [7]). Such II–VI islands are too large as compared to Bohr-

* Corresponding author. Tel.: +49-30-314-22073; fax: +49-30-314-22569.
*E-mail address:* leden@sol.physik.tu-berlin.de (N.N. Ledentsov)
[1] Also at A.F. Ioffe Physical Technical Institute, St. Petersburg, Russia.

0040-6090/00/$ - see front matter 
PII: S0040-6090(00)00659-3

diameter in ZnSe (9 nm [8]) to provide significant quantization. Another way to fabricate quantum wires and QDs has been proposed by using submonolayer (SML) narrow gap insertions in traditional III–V materials systems [9–11]. It was shown that such islands having a height of 1 ML provide a uniform size (width of about 4 nm for InAs elongated islands on GaAs (100) surface) [10]. At the same time the size of the islands of about 4 nm in width and 1 ML in height [10] appears to be insufficient for electron confinement in view of the fairly small electron effective mass. Even in this case the increased exciton binding energy [12] and oscillator strength [13] have been demonstrated. It is clear, on the other hand, that an island of such a size can be used very effectively to localize ZnSe excitons, which have Bohr-radii of about 4.5 nm [8].

The proposal for formation of such islands in case of II–VI SML insertions as well as demonstration of high exciton oscillator strength and lifting of *k*-selection rule for such structures has been given in [14]. This idea, however, was met with criticism, as the mechanisms used for III–V growth were believed to be hardly possible for II–VI materials [15]. However, high-resolution transmission electron microscopy images and studies of the influence of deposition conditions on SML luminescence confirmed formation of nanoscale islands having a lateral size of 4–5 nm [16]. These islands have been revealed both in case of MBE [17] and MOCVD [18] growth. Similar CdSe islands having a two-dimensional (2D) shape and a size of about 7 nm have been recently reported for MBE growth using migration-enhanced MBE mode [19]. Formation of uniform nano-islands can be explained by kinetic [20] or equilibrium models [21,22].

A different interpretation of the CdSe–ZnSe SML growth was given by Toropov et al. [23], who proposed that *uniform quasi-alloy* coverage is formed for CdSe SML depositions for average thickness below 0.7 ML. As opposite, for deposition above 0.7 ML formation of large *mesoscopic islands with dimensions much larger than exciton Bohr-radii* is proposed. The density of these islands has believed to be about $3 \times 10^9$ cm$^{-2}$ and the size is of 20–60 nm [4].

As all basic properties of the laser (modal gain, lasing mechanism, screening of excitons, lifting of **k**-selection rule) are crucially dependent on size density and relative arrangement of islands, it is very important to understand the true nature of SML growth and optical properties of SML structures.

## 2. Self-organization of two-dimensional islands

Spontaneous formation of ordered arrays of islands has been long studied theoretically and experimentally (see e.g. review in Ref. [24]). The formation of ordered ('parquet') structures on crystal surfaces has been shown to occur when two phases with different values of intrinsic surface stress ($\tau_{ij}$) are coexisting on the surface [25]. For strained above-monolayer-high 2D islands having a two-dimensional shape the total energy minimum for particular island size always exists as it was stressed in [26].

In the case of stacked arrays of 2D nano-islands it was predicted that correlated growth prevails at small spacer layer thicknesses, while anticorrelated growth occurs for thicker spacers [27]. This effect has been observed experimentally using processed high-resolution transmission electron microscopy [28]. On the contrary, in publications by Toropov et al. [23,29], anticorrelated growth of mesoscopic islands has been claimed for a new luminescence line evolving for small spacer layer thicknesses.

## 3. Structural characterization of ultrathin insertions

Processed high-resolution transmission electron microscopy (HRTEM) arises as a powerful tool to reveal the structural properties of structures with ultrasmall QDs. In Fig. 1 we show a processed HRTEM image obtained using DALI procedure [30] for a stacked SML–CdSe/ZnMgSSe structure with 30 Å spacer thickness. A color-coded map corresponding to the local lattice parameter in growth direction is shown. The image was taken by a projection of a relatively thick foil of 12–20 nm, where many islands are captured. Similar contrast has been revealed for a SML-CdSe/ZnSe structure with the same spacer thickness [17]. The image reveals planar islands with a lateral size of only a few nanometres. According to the larger island size distribution in the case of quaternary matrix, the full width at half-maximum (FWHM) of the PL band is broader [31] than observed for ZnSe matrix [17]. At the same time quaternary material having a wider bandgap provides larger QD localization energy.

In the case of CdSe/ZnSe structures HRTEM investigations were performed for samples with different spacer thicknesses [28,32,33]. Here, a correlated growth of islands was observed for spacer layer thickness $<3$ nm, while anticorrelated growth occurs for spacers thicker than 3 nm. The lateral size of the QDs is about 4–5 nm in the case of ZnSe matrix. Essentially the same size of the CdSe island has been revealed in Ref. [19]. For MOCVD-grown QDs the lateral size varies between 2 and 6 nm and, thus, the PL emission from ultrathin (0.5–2 ML) insertions is broader [34]. We found no principal difference in the island size and shape in cases of the average CdSe thickness below or slightly above 1 ML.

## 4. Emission of individual QDs

Three-dimensional (3D) confinement of excitons at 2D nano-islands must produce an atom-like energy spectrum of excitons [35] leading to the appearance of discrete energy levels of QDs. In the case of a very dense array of QDs, e.g. as formed by ultrathin insertions, it is very difficult to resolve luminescence lines corresponding to individual

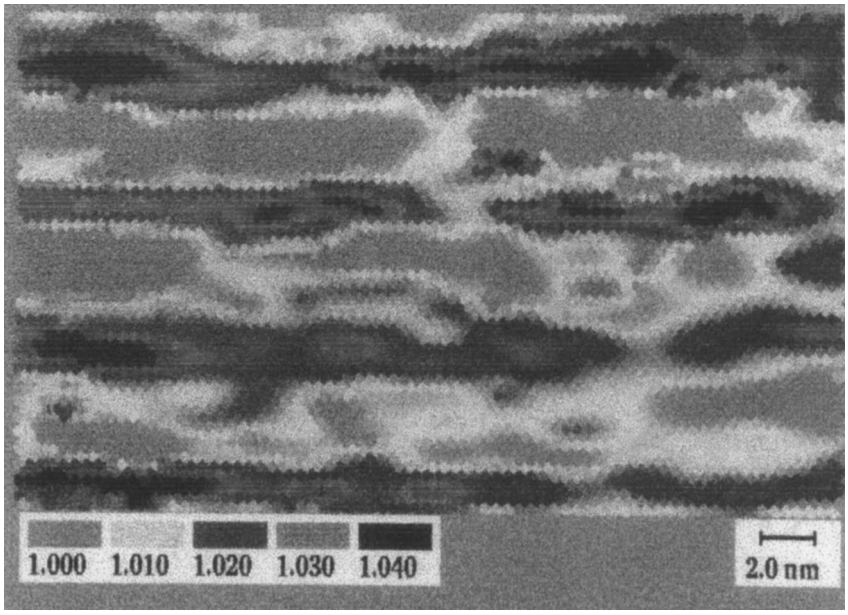


Fig. 1. The color-coded map of the local lattice parameter (LLP) in growth direction digitally processed from a HRTEM image of a stacked submonolayer-CdSe/ZnMgSSe structure with 3 nm spacer thickness.

QDs. Such a result has been achieved in spot-focus cathodoluminescence (CL) studies. The luminescence spectrum of a MOVPE-grown sample [34] with a ~1 ML CdSe insertion in a ZnSSe matrix is depicted in Fig. 2. The FWHM of the sharp emission lines, corresponding to spatially resolved luminescent areas, are limited by the spectral resolution of the setup. Ultrasharp luminsescence lines due to single QDs and a high density of nanoscale QDs formed by 1–2 ML CdSe deposition in a ZnSe matrix using MBE-growth has been proven using etched mesas in Ref. [19].

## 5. Polarization of edge emission and symmetry of the heavy hole wavefunction in QDs

Polarization of the luminescence in edge geometry enables a clear distinction between the QW and QD cases. According to Kane's selection rule, the heavy hole exciton luminescence in QWs must be completely TE polarized. As opposite to the QW case, a significant contribution of TM emission has been observed (Fig. 3), pointing to a significant role of exciton lateral confinement. The most remarkable observation has been done for polarization of edge emission in case of vertically-coupled QD states (see Fig. 3c). This emission is predominantly TM polarized. This indicates that the heavy-hole wavefunction is more extended in the growth direction and a has rippled-cigar shape. A similar effect has been observed in case of vertically-coupled InGaAs–GaAs Stranski–Krastanow QDs with large number of stacks [36].

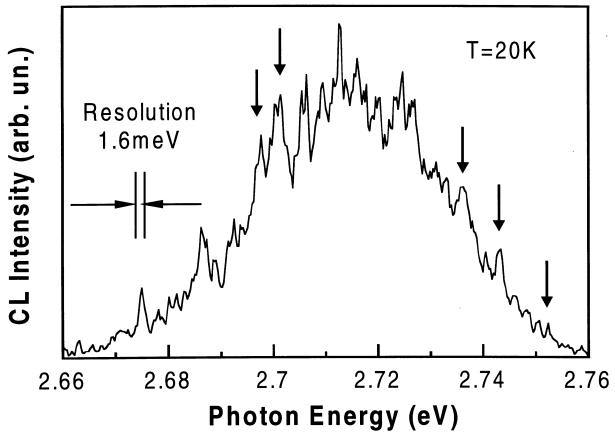


Fig. 2. Cathodoluminescence (CL) spectra of single 1 ML CdSe insertion in a ZnSSe at $T = 20$ K. The sharp luminescence lines in the spectra originate from single QDs.

The extension of the exciton wavefunction in uncoupled and coupled QD structures was estimated from the Zeeman behavior with B applied parallel to the growth direction [37]. The lateral extension of the exciton wavefunctions, estimated following Ref. [38] from the diamagnetic shifts, are ~5.5 nm and <3 nm for uncoupled and coupled QDs, respectively, being much smaller then the bulk Bohr-diameter (9 nm) [8]. These results are in good agreement with the lateral dimensions of the 2D islands observed in cross-sectional HRTEM images [28], supporting the corresponding localization of the excitons. Smaller lateral size of the coupled islands revealed in Ref. [28] explains non-monotonous behavior of the corresponding PL peak with a decrease in the spacer layer thickness (see Fig. 3b,c).

## 6. Matrix effects: lack of QD exciton transport in the case of wide-gap matrix

Despite of the observation of luminescence lines due to single QDs, high density of QDs may result in efficient

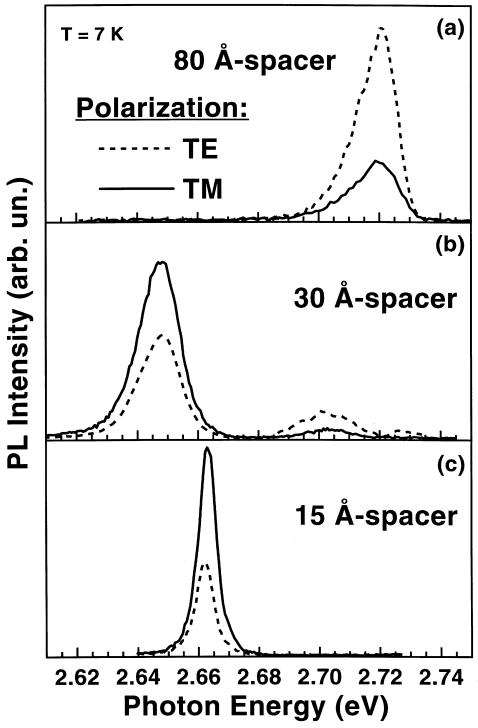


Fig. 3. Linearly polarized photoluminescence (PL) of structures with 80 (a), 30 (b) and 15 Å (c) spacers measured in edge geometry. The polarization changes from mostly TE for uncoupled islands (80 Å spacers) to mostly TM (accompanied by a red shift) for vertically coupled islands (15 Å spacers). The 30 Å spacer sample shows emission from both types of islands.

energy transfer processes in lateral and vertical directions. This results in a predominant tunneling to neighboring larger QDs, having lower exciton transition energy, similar to the case of neighboring thicker and thinner quantum wells. Thus, ground state transitions can be revealed in PLE spectra [32]. This is very different from the case of InAs–GaAs Stranski–Krastanow QDs, where ground state transition is not resolved in PLE spectra, while it is observed in absorption and luminescence spectra [39]. It was observed, however, that by cladding QDs by a wider-gap ZnMgSSe matrix, one can suppress tunneling of excitons and thus realize a true QD-like PLE spectrum [31]. In this case the first peak in PLE spectrum coincides with the first excited state in QD.

## 7. Lasing mechanism in II–VI QDs

In bulk material direct radiative recombination of excitons with finite $k$-vector, which dominate at high temperatures and high excitation densities, is forbidden. Another particle, usually a LO-phonon, is necessary to accommodate the exciton $k$-vector [40]. Thus, exciton–phonon scattering processes dominate the gain mechanism in II–VI materials, where exciton Bohr-radii are small and densities necessary to screen excitons are higher than the excitation density at gain threshold [41]. At even higher excitation densities, exciton–exciton and exciton–electron scattering processes dominate. These processes shift the lasing wavelength typically by one or two LO-phonon energies towards longer wavelength as compared to exciton energy revealed in the absorption spectrum. In QDs, however, the lasing mechanism must have a principally excitonic (or biexcitonic) character, as excitons cannot be screened in QDs and the $k$-selection rule is not appropriate. The excitonic (resonant to QD exciton ground state) character of lasing in CdSe–ZnSe QDs formed by SML deposition was experimentally proved in Ref. [14].

## 8. Resonant waveguiding and lasing

High exciton oscillator strength in case of stacked dense arrays of QDs and the experimentally proven resonant character of lasing stimulated an idea of creating a new type of a laser based on the concept of resonant waveguiding and lasing. Some enhancement of the refractive index originates on the low energy side of the exciton absorption spectrum in II–VI multiple quantum well structures in accordance with Kramers–Kronig relations (see e.g. Ref. [42]), as also in the case of III–V quantum wells. This fact, taken together with reduced screening of excitons in II–VI quantum wells, potentially enables waveguiding in a small spectral window without using of external waveguides. However, long-wavelength shift of the lasing emission away from the exciton resonance region and moderate values of the enhancement in refractive index [42] limit the device application of this effect in quantum wells. At the same time, absorption measurements [43] demonstrated maximum exciton absorption coefficients of the order of $10^5$ $cm^{-1}$ in the case of stacked SML QDs. This fact agrees with the estimation of the exciton oscillator strength from the optical reflectance spectra and correspond to the values of the refractive index enhancement of about 0.2–0.3. QD lasers based on the effect of resonant waveguiding were demonstrated to be exceptionally promising both for II–VI [31] and III–V [44,45] SML structures. This concept allows to bypass the double-heterostructure laser concept, if no lattice-matched heterojunction with significantly lower refractive index exists (e.g. diamond, silicon, etc.).

## 9. Surface lasing without Bragg mirrors and self-adjustment of cavity

High exciton absorption coefficients in arrays of QDs allow to achieve lasing in case of very short cavity lengths in edge geometry, or even realize surface lasing in vertical geometry when no highly-reflecting Bragg mirrors are used. For example, just ZnSe/GaAs and ZnSe/air interfaces allowing to achieve about 30% reflectivity each made it possible to have surface lasing in structures with 20-fold stacked CdSe SML insertions [32]. The surface emission in dependence of

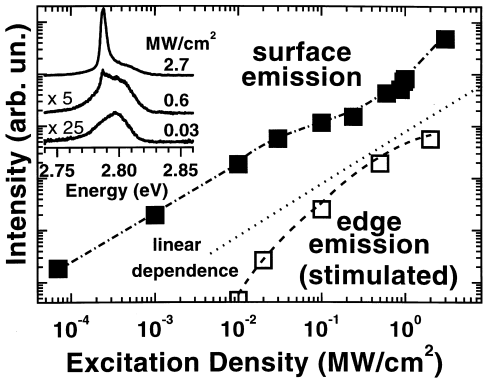


Fig. 4. Surface and edge emission of a stacked SML–CdSe structure with ZnMgSSe barriers as a function of the excitation density. The spectra are vertically displaced for clarity. The superlinear growth and the narrowing of the surface emission occurs, when edge emission saturates. The inset shows the surface emission.

the excitation density is depicted in Fig. 4. One can see from the figure that at low excitation densities, the PL intensity recorded from surface of the structure increases linearly with excitation density. At some density, however, stimulated emission in edge geometry starts, being revealed by narrowing of the PL line and by superlinear growth of the integral PL intensity (see Fig. 4). At these excitation densities, the growth of the PL intensity in the surface direction becomes sublinear. At even higher excitation densities, a sharp peak in the surface PL appears exhibiting pronounced superlinear growth (see inset in Fig. 4). This points to a lasing in the vertical direction. Accordingly, stimulated emission in edge geometry saturates at these excitation densities.

One can conclude from these observations that the main obstacle to obtain surface lasing can be related to stimulated emission in edge geometry, where losses are usually much lower. The total radiative lifetime decreases, leading to pinning of the quasi-Fermi energies for electrons and holes. However, at least at low and moderate temperatures, QD population is not completely described by thermal equilibrium [1], and some increase in the probability of the radiative recombination with excitation density occurs. This finally leads to a situation when gain in the vertical direction overcomes external losses due to small reflectivity of GaAs/ZnSe and ZnMgSSe/air interfaces, and lasing in the vertical direction develops. In this case most of the light comes out in the vertical direction, and the stimulated emission in edge geometry saturates.

In the case when the gain in the active medium is small, the modulation of refractive index, caused by changing gain with increase in the excitation density (chirp) is small. If the gain is high, then the shift of the cavity modes with the excitation density increase can be very significant [32]. This allows achievement of a self-adjustment effect between the cavity mode and the gain spectrum. In this case the cavity mode wavelength tunes with excitation density rise, until it reaches the spectral region, where gain is able to overcome external losses.

Recently a photopumped GaN-based surface emitting laser, emitting in the blue spectral range, has been realized using a similar concept [46]. The structure was grown by MOCVD and comprised a 2.5-μm-thick GaN layer followed by an active region. This region consisted of a 25-nm-thick relaxed InGaN layer with a low indium content (10% In) followed by a strain-compensated multilayer InGaN–GaN structure composed of 12 periods and having the same average In content. The multilayer structure was formed by temperature cycling between 730 and 860°C, resulting in a modulated In compositional profile, as the In incorporation is strongly affected by substrate temperature. A 0.1-μm-thick GaN cap layer was deposited on top.

Low-temperature photoluminescence, lasing and optical transmission spectra, all in the direction perpendicular to the sample surface, are shown in Fig. 5. The PL spectrum shows a single relatively broad peak with extended tails on both high and low energy sides. This, together with a significant energy shift between the PL maximum and the onset of the pronounced InGaN absorption in the transmission spectra, agree with formation of In-rich nanodomains with significant size dispersion as revealed in HREM (about 1.5–5 nm). At large excitation densities, PL intensity maximum shifts to higher photon energies, narrows, and its intensity superlinearly increase with excitation density (see Fig. 5, inset). These effects taken together point to observation of stimulated emission in surface geometry. We note that the PL maximum, also in the latter case, remains in the very vicinity of the onset of the absorption induced by the InGaN insertions.

The dependence of the PL intensity on excitation density at 150 K is shown in Fig. 6a. PL spectra for different excitation densities are shown in Fig. 6b. The reduced differential efficiency of the stimulated emission at higher temperatures makes the spectral changes related to the increase in excitation density more evident. It can be seen from the Fig. 6 that

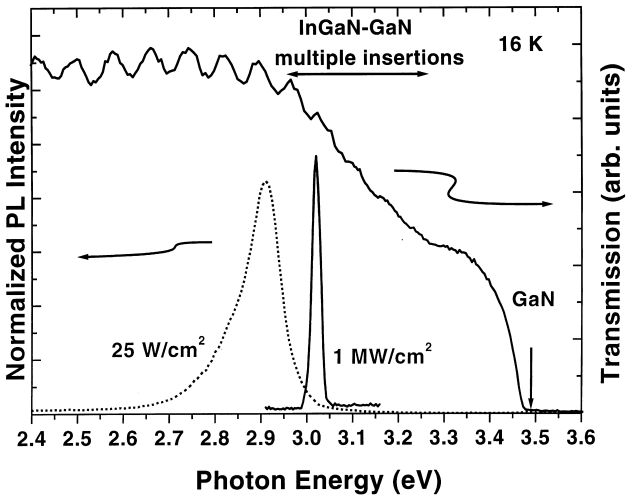


Fig. 5. Low-temperature PL spectra at low and high excitation densities and optical transmission spectrum of the structure. PL intensity vs. excitation density is shown in the inset.

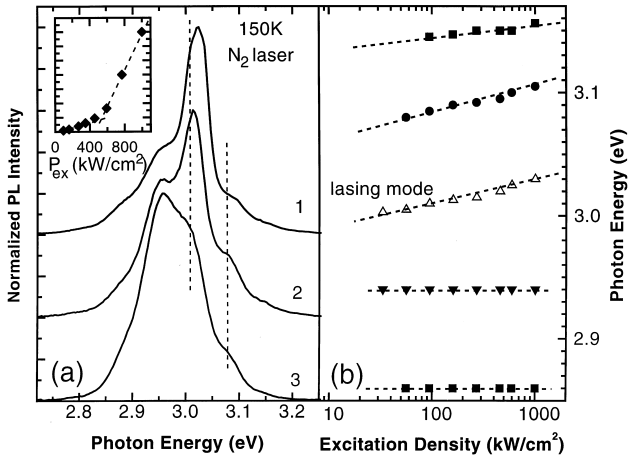


Fig. 6. (a) PL spectra at different excitation densities 1, 1 MW/cm$^2$; 2, 0.59 MW/cm$^2$; 3, 0.16 MW/cm$^2$ (PL intensity vs. excitation density is shown in the inset). (b) Cavity mode energies vs. excitation density.

all the PL spectra are modulated by the modes of the Fabry–Perot microcavity formed by the GaN/$Al_2O_3$ interface and the GaN surface. It is clearly seen that at high excitation densities (>600 kW/cm$^2$) one of the cavity modes starts to dominate in the PL spectra and its peak intensity grows superlinearly. Single-mode emission together with a strong increase in the slope efficiency indicates the presence of the feedback in the system despite of the remarkably low finesse of the cavity. This is a clear demonstration of lasing in vertical direction for structures with stacked InGaN insertions, and a first demonstration of the possibility to reach surface lasing in group III nitrides without using of high-reflectivity Bragg mirrors.

Using of bottom AlGaN/GaN Bragg reflector allowed achievement of room temperature surface lasing [47]. DBRs with maximum reflectivity exceeding 90% can be realized using AlGaN–GaN strain-compensated growth on top of the AlGaN buffer layer [47]. The current geometry of VCSEL did not imply a top DBR (GaN/air interface played this role). Nevertheless, as was already mentioned, ultrahigh material gain in stacked InGaN insertions made it potentially possible to achieve surface lasing even in case of very low finesse cavities. Room-temperature PL spectra of the VCSEL structure recorded at different excitation densities are shown in Fig. 7. A strong increase in slope efficiency (see inset in Fig. 7) and narrowing of the PL line confirms lasing. The same conclusion can be driven from the far-field pattern of the emission. The room-temperature threshold excitation density was 400 kW/cm$^2$. We note that the lasing emission appears on the long-wavelength side of the PL spectra. Thus the lasing occurs via localized states caused by In-rich nanodomains formed in the InGaN insertions. On the contrary, it was shown that structures grown without the bottom DBR lase on a high energy side of the PL spectra (see Fig. 5) due necessity to achieve higher gain to overcome larger external optical losses.

## 10. Realization of green emission using ultrathin InGaN–GaN insertions

As it was already pointed out, large effective masses of charge carriers in wide-gap matrices allow large localization energies of excitons also in the case of ultrathin insertions of narrow-gap material. Transmission electron microscopy image of multiple InGaN–GaN insertions in a GaN matrix emitting in the green spectral range is shown in Fig. 8a. The average thickness of the InGaN insertions is about two monolayers in this case. Gain spectra measured in the same structure is shown in Fig. 8b. With excitation density rise, first peaks in the green spectral range develop, then the ground state emission saturates, and new peaks appear on the high energy side. There is no shift of the peaks with the excitation density rise, and only their relative intensity changes. This rules out significant importance of piezoelectric effects. Despite the fact that stimulated emission in this structure develops only in the blue spectral range, a significant relative gain in the green spectral range is also observed [48]. This demonstrates a possibility to achieve green lasing using ultrathin InGaN insertions, avoiding defects due to thick layers of lattice mismatched InGaN, and reducing a negative impact of piezoelectric fields.

## 11. Conclusion

To conclude, we discussed optical properties of ultrathin insertions in wide-gap matrices. These insertions represent dense arrays of two-dimensional nano-islands with a size comparable to the exciton Bohr-radius, as follows from the transmission electron microscopy studies. The QD nature is proven by direct observation of luminescence lines from single QDs, by resonant character of gain, by lateral squeezing of excitons revealed in magneto-optical studies, and by polarization of the QD emission. Very

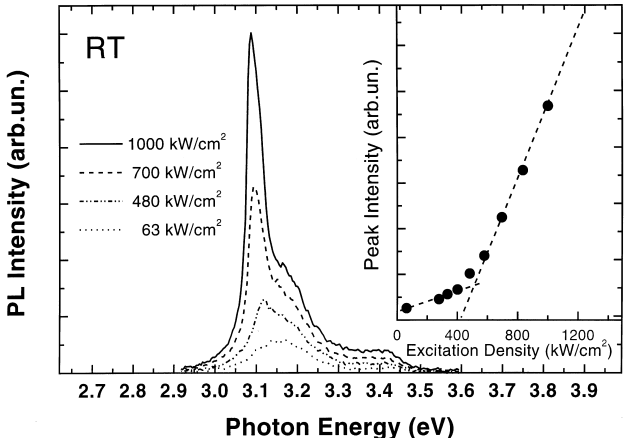


Fig. 7. Room-temperature photoluminescence (PL) spectra of the VCSEL structure at different excitation densities (solid line, 1000 kW/cm$^2$; dashed line, 700 kW/cm$^2$; short dashed line, 480 kW/cm$^2$; dotted line, 63 kW/cm$^2$). Inset shows dependence of the peak PL intensity on excitation density.

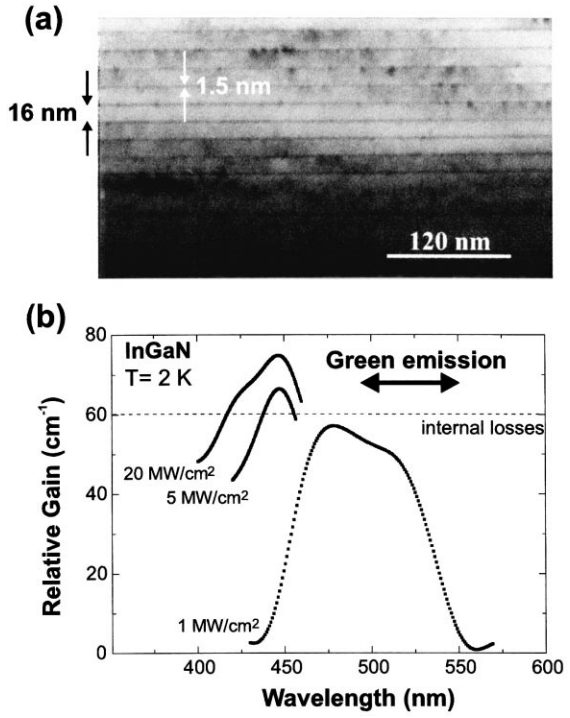


Fig. 8. (a) Transmission electron microscopy image of multiple InGaN–GaN insertions in a GaN matrix emitting in the green spectral range. The average thickness of the InGaN insertions is only about two monolayers. (b) Gain spectra measured in the same structure. Note the significant relative gain in the green spectral range.

recently a new effect of polarization splitting of the gain band in QDs was predicted and observed [49]. New effects led to fabrication of unique devices such as resonantly-waveguiding lasers and cavity-self-adjusted surface-emitting lasers without Bragg reflectors. Despite most of these effects being applied to QDs based on wide-gap compounds, some of the effects are realized in QDs based on conventional III–V materials. Resonant waveguiding and lasing has been demonstrated for InAs submonolayer insertions in an AlGaAs matrix [44,45]. Self-adjustment of the gain spectrum and the cavity mode has been observed for vertical cavity lasers using vertically-coupled InGaAs–GaAs QDs as an active medium [50].

## Acknowledgements

This work was supported by the Russian Foundation on Basic Research, NATO SfP 972614 grant, Deutsche Forschungsgemeinschaft (DFG) and the Program of Ministry of Science of Russian Federation 'Physics of solid-states nanostructures'. We gratefully acknowledge S.V. Ivanov and S.V. Sorokin for expert MBE growth of II–VI structures. N.N.L. is supported by a Guest Professorship Program of DAAD.

## References

[1] D. Bimberg, M. Grundmann, N.N. Ledentsov, Quantum Dot Hetrerostructures, Wiley, Chichester, 1999, p. 328.
[2] U. Woggon, O. Wind, F. Gindele, E. Tsitsishvili, M. Müller, J. Lumin. 70 (1996) 269.
[3] Yu.M. Shernyakov, D.A. Bedarev, E.Yu. Kondrat'eva, et al., Electron. Lett. (2000) in press.
[4] S.V. Ivanov, A.A. Toropov, S.V. Sorokin, et al., Appl. Phys. Lett. 74 (1999) 498.
[5] S. Nakamura, M. Senoh, S. Nagahama, et al., Appl. Phys. Lett. 70 (1997) 2753.
[6] J. Gutowski, U. Neukirch, P. Michler, B. Haase, K. Wundke, J. Cryst. Growth 184/185 (1998) 1.
[7] M. Arita, A. Avramescu, K. Uesugi, et al., Jpn. J. Appl. Phys. 36 (1997) 4097.
[8] J. Puls, M. Rabe, A. Siarkos, F. Henneberger, Phys. Rev. B 57 (1998) 14749.
[9] O. Brandt, H. Lage, G.C. La Rocca, A. Heberle, K. Ploog, Surf. Sci. 267 (1992) 319.
[10] V. Bressler-Hill, A. Lorke, S. Varma, P.M. Petroff, K. Pond, W.H. Weinberg, Phys. Rev. B 50 (1994) 8479.
[11] P.D. Wang, N.N. Ledentsov, C.M. Sotomayor Torres, P.S. Kop'ev, V.M. Ustinov, Appl. Phys. Lett. 64 (1994) 1526.
[12] P.D. Wang, N.N. Ledentsov, C.M. Sotomayor Torres, et al., Phys. Rev. B 50 (1994) 1604.
[13] M.V. Belousov, N.N. Ledentsov, M.V. Maximov, et al., Phys. Rev. B 51 (1995) 14346.
[14] N.N. Ledentsov, I.L. Krestnikov, M.V. Maximov, et al., Appl. Phys. Lett. 69 (1996) 1343.
[15] K.P. O'Donnel, U. Woggon, Appl. Phys. Lett. 70 (1997) 2765.
[16] N.N. Ledentsov, I.L. Krestnikov, M.V. Maximov, et al., Appl. Phys. Lett. 70 (1997) 2766.
[17] M. Strassburg, V. Kutzer, U.W. Pohl, et al., Appl. Phys. Lett. 72 (1998) 942.
[18] U.W. Pohl, R. Engelhardt, V. Türck, D. Bimberg, J. Cryst. Growth 195 (1998) 569.
[19] T. Kümmell, R. Weigand, G. Bacher, et al., Appl. Phys. Lett. 73 (1998) 3105.
[20] V. Bressler-Hill, S. Varma, A. Lorke, B.Z. Nosho, P.M. Petroff, W.H. Weinberg, Phys. Rev. Lett. 74 (1995) 3209.
[21] N.N. Ledentsov, M. Grundmann, N. Kirstaedter, et al., Solid State Electron. 40 (1996) 785.
[22] V.A. Shchukin, N.N. Ledentsov, M. Grundmann, D. Bimberg, in: G. Abstreiter, A. Aydinli, J.-P. Leburton (Eds.), Optical Properties of Low Dimensional Semiconductors, *NATO ASI Series. Series E: Applied Sciences*, 344, Kluwer, Dordrecht, 1997, p. 257.
[23] A.A. Toropov, S.V. Ivanov, T.V. Shubina, et al., J. Cryst. Growth 293 (1998) 184/185.
[24] V.A. Shchukin, D. Bimberg, Rev. Mod. Phys. (2000) in press.
[25] V.I. Marchenko, JETP Lett. 33 (1981) 381.
[26] J. Tersoff, R.M. Tromp, Phys. Rev. Lett. 70 (1993) 2782.
[27] V.A. Shchukin, D. Bimberg, V.G. Malyshkin, N.N. Ledentsov, Phys. Rev. B 57 (1998) 12262.
[28] M. Strassburg, I.L. Krestnikov, A. Göldner, et al., in: D. Gershoni, et al. (Eds.), *Proc. 24th Int. Conf.: Physics of Semiconductors*, Jerusalem, Israel, August 2–7, 1998, World Scientific, Singapore, 1999.
[29] A.A. Toropov, T.V. Shubina, S.V. Sorokin, et al., Phys. Rev. B 59 (1999) R2510.
[30] A. Rosenauer, S. Kaiser, T. Reisinger, J. Zweck, W. Gebhardt, D. Gerthsen, Optik 102 (1996) 63.
[31] I.L. Krestnikov, M.V. Maximov, A.V. Sakharov, et al., J. Cryst. Growth 545 (1998) 184/185.
[32] I.L. Krestnikov, M. Straßburg, M. Caesar, et al., Phys. Rev. B (2000) in press.
[33] I.L. Krestnikov, M. Strassburg, M. Caesar, et al., in: D. Gershoni, et al. (Eds.), *Proc. 24th Int. Conf.: Physics of Semiconductors*,

Jerusalem, Israel, August 2–7, 1998, World Scientific, Singapore, 1999.
[34] R. Engelhardt, V. Türck, U.W. Pohl, D. Bimberg, J. Cryst. Growth 311 (1998) 184/185.
[35] M. Grundmann, J. Christen, N.N. Ledentsov, et al., Phys. Rev. Lett. 74 (1995) 4043.
[36] P. Yu, J. Hvam, N.N. Ledentsov, V.M. Ustinov, D. Bimberg, Phys. Rev. B (2000) in press.
[37] M. Straßburg, R. Heitz, V. Türck, et al., J. Electron. Mater. (2000) in press.
[38] I.E. Itskevich, M. Henini, H.A. Carmona, L. Eaves, P.C. Main, D.K. Maude, J.C. Portal, Appl. Phys. Lett. 70 (1997) 505.
[39] N.N. Ledentsov, N. Grundmann, M. Kirstaedter, et al., in: D.J. Lockwood, et al. (Eds.), Proc. 22nd Int. Conf.: Physics of Semiconductors, Vancouver, Canada, 1994, Vol. 3, World Scientific, Singapore, 1995, p. 1855.
[40] E. Gross, S. Permogorov, A. Razbirin, J. Phys. Chem. Solids 27 (1966) 1647.
[41] C. Benoit a la Guillaume, J.M. Denber, F. Salvan, Phys. Rev. 177 (1969) 567.
[42] Zh.I. Alferov, S.V. Ivanov, P.S. Kop'ev, et al., Superlattices Microstructures 15 (1994) 65.
[43] G.N. Aliev, A.D. Andreev, R.M. Datsiev, et al., J. Cryst. Growth 315 (1998) 184/185.
[44] N.N. Ledentsov, A.F. Tsatsul'nikov, A.Yu. Egorov, et al., Appl. Phys. Lett. 74 (1999) 161.
[45] B.V. Volovik, A.Yu. Egorov, P.S. Kop'ev, et al., in: D. Gershoni, et al. (Eds.), *Proc. 24th Int. Conf.: Physics of Semiconductors*, Jerusalem, August 2–7, 1998, World Scientific, Singapore, 1999.
[46] A.V. Sakharov, W.V. Lundin, I.L. Krestnikov, et al. (2000) in press.
[47] I.L. Krestnikov, W.V. Lundin, A.V. Sakharov, et al. (2000) in press.
[48] A.V. Sakharov, et al., Proc. ICNS (2000) in press.
[49] G.Ya. Slepyan, S.A. Maksimenko, V.P. Kalosha, et al., Phys. Rev. B 59 (1999) 12275.
[50] N.N. Ledentsov, D. Bimberg, V.M. Ustinov, et al., Semicond. Sci. Technol. 13 (1999) 99.